Radii and spectroscopy of medium-mass nuclei from Green's Function theory

Laser spectroscopy as a tool for nuclear theories
(7-11 October 2019, CEA)

Francesco Raimondi

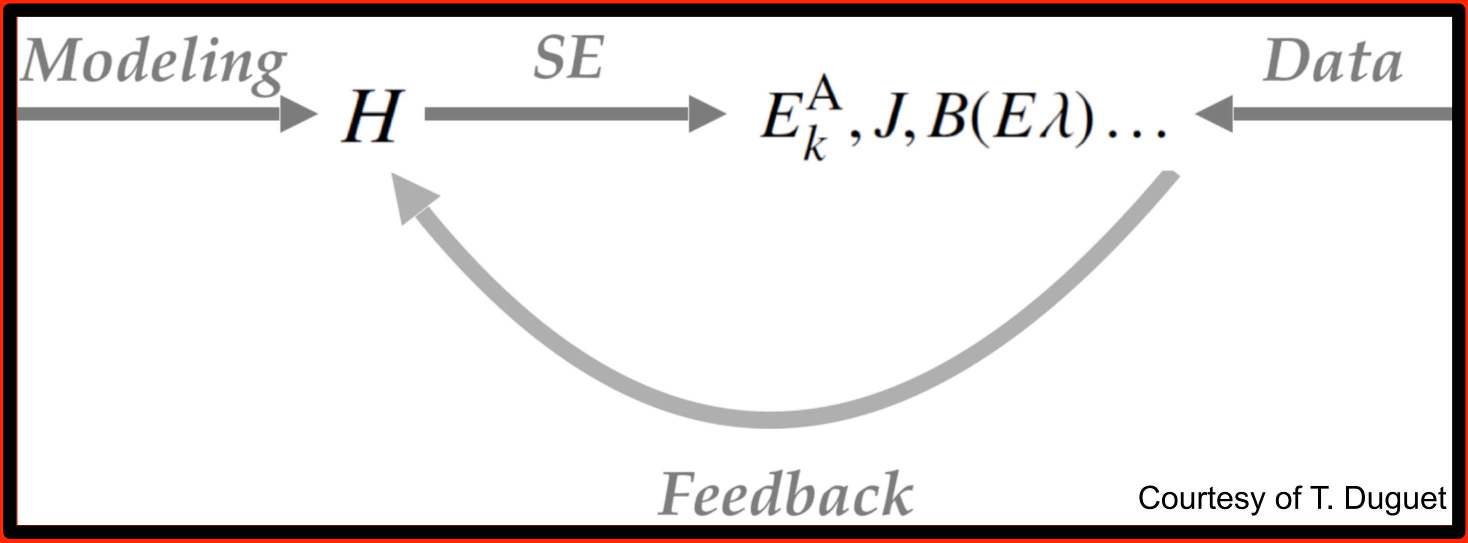

Courtesy of T. Duguet

Outline

- Self-consistent Green's function (SCGF) method

  Recent pedagogical review: A. Carbone, C. Barbieri, *Lect. Notes Phys.* 936 (2017)

- Testing χEFT Hamiltonians with SCGF

  V. Somà, P. Navrátil, FR, C. Barbieri, T. Duguet, *arXiv: 1907.09790* (2019)

  - Radii of Oxygen, Calcium and Nickel isotopic chains
  - Spectra of selected Calcium and Potassium isotopes

- Dipole Response Function and Polarisability in medium mass nuclei

  FR, C. Barbieri, *Phys. Rev. C* **99** 054327 (2019)

  - Oxygen isotopes: ^{14}O, ^{16}O, ^{22}O and ^{24}O
  - Calcium isotopes: ^{36}Ca, ^{40}Ca, ^{48}Ca and ^{54}Ca
  - ^{68}Ni

Ab initio methods based on many-body expansion

A-body Schrödinger equation

$$\mathcal{H}\,|\Psi_n^A\rangle = E_n^A\,|\Psi_n^A\rangle$$

A-body Hamiltonian

$$\mathcal{H} = T + V^{2N} + V^{3N} + V^{4N} + \cdots + V^{AN}$$

A-body wave function

$$|\Psi_n^A\rangle, \quad \langle\Psi_n^A|\mathcal{O}|\Psi_n^A\rangle$$

Realistic interaction:

- QCD-based (χEFT)
- Truncated at 3N level
- Main source of theoretical error in nuclei computation

Expansion around a reference state:

- Uncorrelated mean-field reference state
- Include correlations via symmetry-breaking and/or *np-nh* excitations
- Truncated but systematically improvable
- Resummed beyond perturbative regime

SCGF

Coupled cluster theory

MBPT

In-medium SRG theory

Self-consistent Green's function formalism

A-body Schrödinger equation

$$\mathcal{H} \, |\Psi_n^A\rangle = E_n^A \, |\Psi_n^A\rangle$$

Introduce 1-body, 2-body, … A-body quantities (Green's functions)

$$i\,\mathcal{G}_{ab}^{1b}(t,t') \equiv \langle\Psi_0^A| T\left\{a_a(t)a_b^\dagger(t')\right\}|\Psi_0^A\rangle$$

Energy and one-body observables

Expansion around a reference state (A conserved)

$$\mathcal{H} = \mathcal{H}_0 + \mathcal{H}_1$$

$$|\Phi_0^A\rangle \qquad |\Psi_0^A\rangle = \hat{\Omega}\,|\Phi_0^A\rangle$$

Wave operator

Dyson equation

$$\mathcal{G}_{ab}(\omega) = \mathcal{G}_{ab}^{(0)}(\omega) + \sum_{cd} \mathcal{G}_{ac}^{(0)}(\omega)\,\tilde{\Sigma}_{cd}(\omega)\,\mathcal{G}_{db}(\omega)$$

Self-energy: effective potential affecting the s.p. propagation in the nuclear medium

Self-energy expansion and resummation

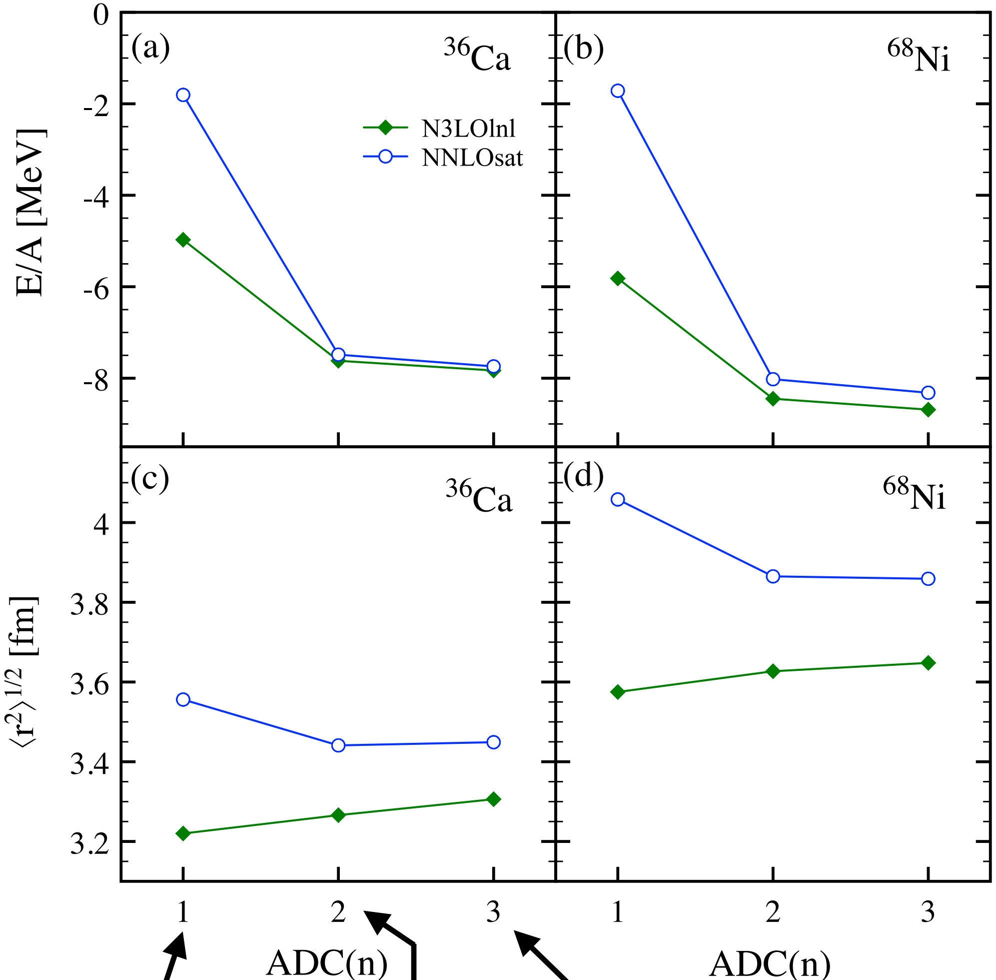

Nonperturbative resummation

Algebraic Diagrammatic Construction ADC(N)

J. Schirmer
Phys. Rev. A26, 2395 (1982)
Phys. Rev. A28, 1237 (1983)

Classes of diagrams (ladder and ring) summed at infinite order by means of a geometric series

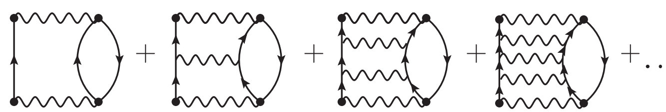

(resummed at ADC(3))

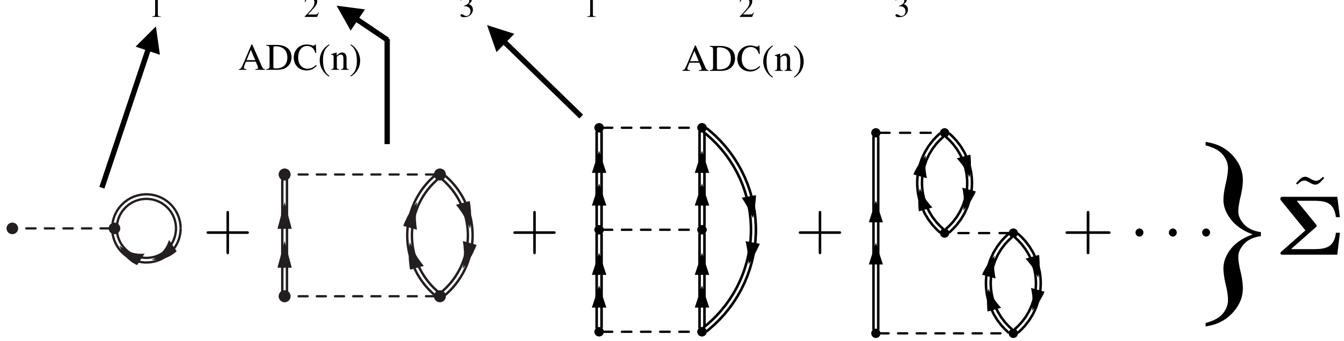

Expansion organised in Feynman diagrams

Gorkov-Green's functions for open-shell systems

Open-shell systems:
zero-order degeneracies → Breakdown of many-body perturbation theory (no account of superfluidity)

$$\mathcal{H}\,|\Psi_n^{\cancel{A}}\rangle = E_n^{\cancel{A}}|\Psi_n^{\cancel{A}}\rangle$$

$$|\Psi_0\rangle \equiv \sum_{A}^{\text{even}} c_A\,|\psi_0^A\rangle$$

U(1) symmetry broken (particle number)

$$\Omega = \mathcal{H} - \lambda A$$

Grand potential (λ chemical potential)

Gorkov diagrammatic for SCGF [Somà, Duguet & Barbieri 2011]

$$i\,G_{ab}^{11}(t,t') \equiv \langle\Psi_0|T\left\{a_a(t)a_b^\dagger(t')\right\}|\Psi_0\rangle \qquad i\,G_{ab}^{12}(t,t') \equiv \langle\Psi_0|T\left\{a_a(t)\bar{a}_b(t')\right\}|\Psi_0\rangle$$

$$i\,G_{ab}^{22}(t,t') \equiv \langle\Psi_0|T\left\{\bar{a}_a^\dagger(t)\bar{a}_b(t')\right\}|\Psi_0\rangle \qquad i\,G_{ab}^{21}(t,t') \equiv \langle\Psi_0|T\left\{\bar{a}_a^\dagger(t)a_b^\dagger(t')\right\}|\Psi_0\rangle$$

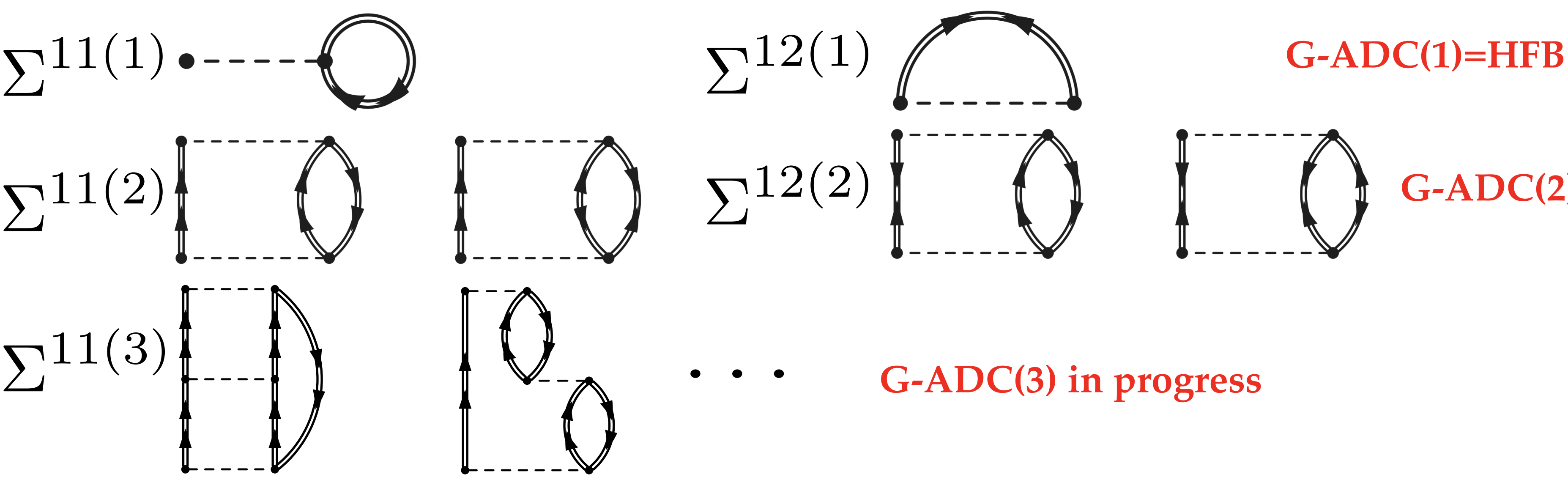

Observables: g.s. energy and one-body operators

Lehmann representation of the one-body Green's function

$$\mathcal{G}^{1b}_{\alpha\beta}(\omega) = \sum_n \frac{\langle\Psi_0^A|a_\alpha|\Psi_n^{A+1}\rangle\langle\Psi_n^{A+1}|a_\beta^\dagger|\Psi_0^A\rangle}{\hbar\omega-(E_n^{A+1}-E_0^A)+i\eta} + \sum_k \frac{\langle\Psi_0^A|a_\beta^\dagger|\Psi_k^{A-1}\rangle\langle\Psi_k^{A-1}|a_\alpha|\Psi_0^A\rangle}{\hbar\omega-(E_0^A-E_k^{A-1})-i\eta}$$

$$\equiv \sum_n \frac{(\mathcal{X}_\alpha^n)^*\mathcal{X}_\beta^n}{\hbar\omega-\varepsilon_n^+ + i\eta} + \sum_k \frac{\mathcal{Y}_\alpha^k(\mathcal{Y}_\beta^k)^*}{\hbar\omega-\varepsilon_k^- - i\eta},$$

Spectroscopic factors

$$SF_k^- = \sum_\alpha |\mathcal{Y}_\alpha^k|^2$$

$$SF_n^+ = \sum_\alpha |\mathcal{X}_\alpha^n|^2$$

$$S^h_{\alpha\beta}(\omega) = \frac{1}{\pi} Im\,\mathcal{G}^{1b}_{\alpha\beta}(\omega)$$

Ground-state Energy (Koltun sum rule)

$$E_0^A = \sum_{\alpha\beta}\frac{1}{2}\int_{-\infty}^{\varepsilon_0^-}[T_{\alpha\beta}+\omega\,\delta_{\alpha\beta}]\,S^h_{\beta\alpha}(\omega)\,\mathrm{d}\omega - \frac{1}{2}\langle\widehat{W}\rangle$$

One-body density matrix/observables

$$\rho_{\alpha\beta} \equiv \langle\Psi_0^A|a_\beta^\dagger a_\alpha|\Psi_0^A\rangle = \int_{-\infty}^{\varepsilon_0^-} S^h_{\alpha\beta}(\omega)\,\mathrm{d}\omega \longrightarrow \langle\widehat{O}^{1B}\rangle = \sum_{\alpha\beta} O^{1B}_{\alpha\beta}\,\rho_{\beta\alpha}$$

Ex: radii, charge distribution

Observables: Excitation spectra

Lehmann representation of the one-body Green's function

$$\mathcal{G}^{1b}_{\alpha\beta}(\omega) = \sum_n \frac{\langle\Psi_0^A|a_\alpha|\Psi_n^{A+1}\rangle\langle\Psi_n^{A+1}|a^\dagger_\beta|\Psi_0^A\rangle}{\hbar\omega-(E_n^{A+1}-E_0^A)+i\eta} + \sum_k \frac{\langle\Psi_0^A|a^\dagger_\beta|\Psi_k^{A-1}\rangle\langle\Psi_k^{A-1}|a_\alpha|\Psi_0^A\rangle}{\hbar\omega-(E_0^A-E_k^{A-1})-i\eta}$$

$$\equiv \sum_n \frac{(\mathcal{X}^n_\alpha)^*\mathcal{X}^n_\beta}{\hbar\omega-\varepsilon^+_n+i\eta} + \sum_k \frac{\mathcal{Y}^k_\alpha(\mathcal{Y}^k_\beta)^*}{\hbar\omega-\varepsilon^-_k-i\eta}\,,$$

One-nucleon addition separation energies

One-nucleon removal separation energies

$$\varepsilon^-_k \equiv E_0^A - E_k^{A-1}$$

$$\varepsilon^+_n \equiv E_n^{A+1} - E_0^A$$

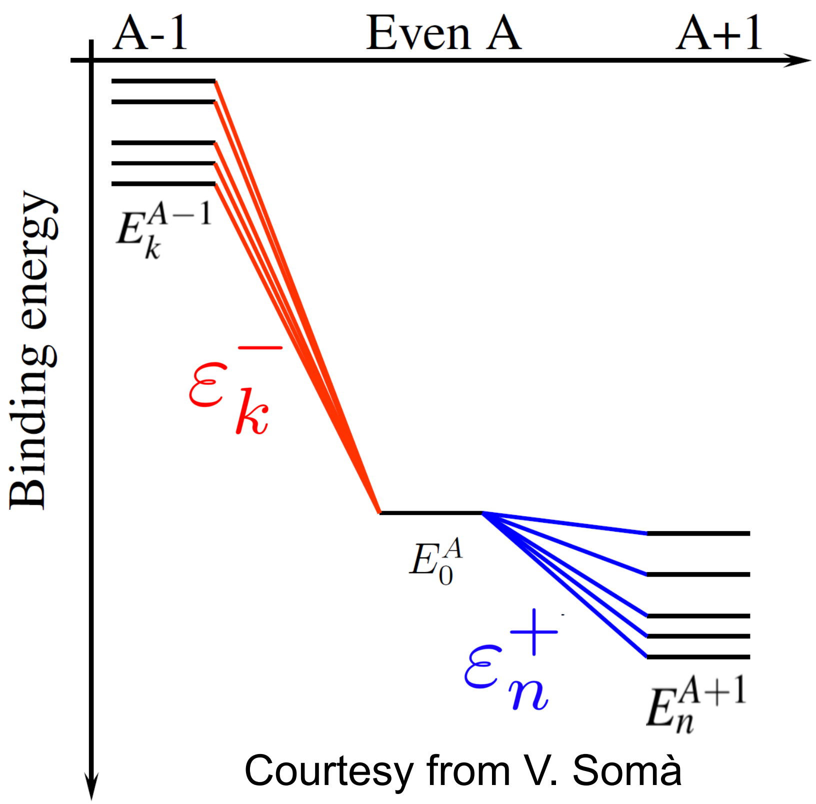

Courtesy from V. Somà

Outline

- Self-consistent Green's function (SCGF) method

  Recent pedagogical review: A. Carbone, C. Barbieri, *Lect. Notes Phys.* 936 (2017)

- Testing χEFT Hamiltonians with SCGF

  V. Somà, P. Navrátil, FR, C. Barbieri, T. Duguet, *arXiv: 1907.09790* (2019)

  - Radii of Oxygen, Calcium and Nickel isotopic chains
  - Spectra of selected Calcium and Potassium isotopes

- Dipole Response Function and Polarisability in medium mass nuclei

  FR, C. Barbieri, *Phys. Rev. C* **99** 054327 (2019)

  - Oxygen isotopes: ^{14}O, ^{16}O, ^{22}O and ^{24}O
  - Calcium isotopes: ^{36}Ca, ^{40}Ca, ^{48}Ca and ^{54}Ca
  - ^{68}Ni

Chiral Hamiltonians

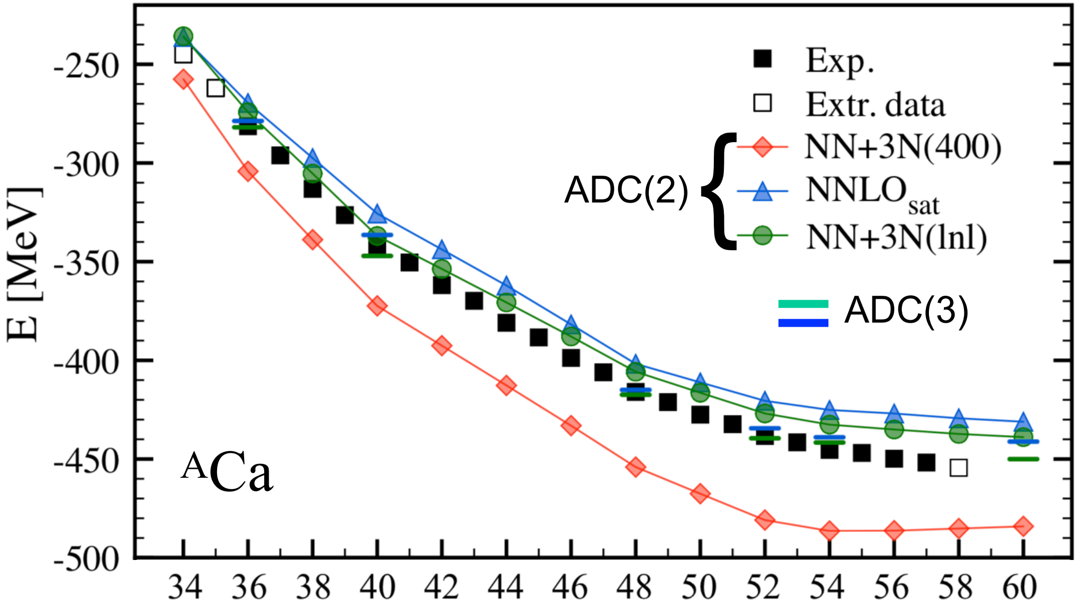

NN+3N(400) (~2010) SRG λ=2.0 fm^{-1}

[Entem & Machleidt 2003, Navrátil 2007]

NNLO$_{sat}$ (2015)

[Ekström *et al.* 2015]

NN+3N(lnl) (2018) SRG λ=2.0 fm^{-1}

[Entem & Machleidt 2003, Navrátil 2018]

χEFT	Expansion	Fit	Regulator	Features
NN+3N(400)	N^{3}LO *NN* + N^{2}LO *3N*	fit *X*-body sector on *X*-body data	Local	Overbinding, Radii too small
NNLO$_{sat}$	N^{2}LO	fit many-body data (O and C)	Local / Nonlocal	BE and radii up to Ca, Few-body syst deteriorated
NN+3N(lnl)	N^{3}LO *NN* + N^{2}LO *3N*	fit *X*-body sector on *X*-body data	Local / Nonlocal	Mid-mass and heavy systems? Radii?

Charge radii in Oxygen isotopes

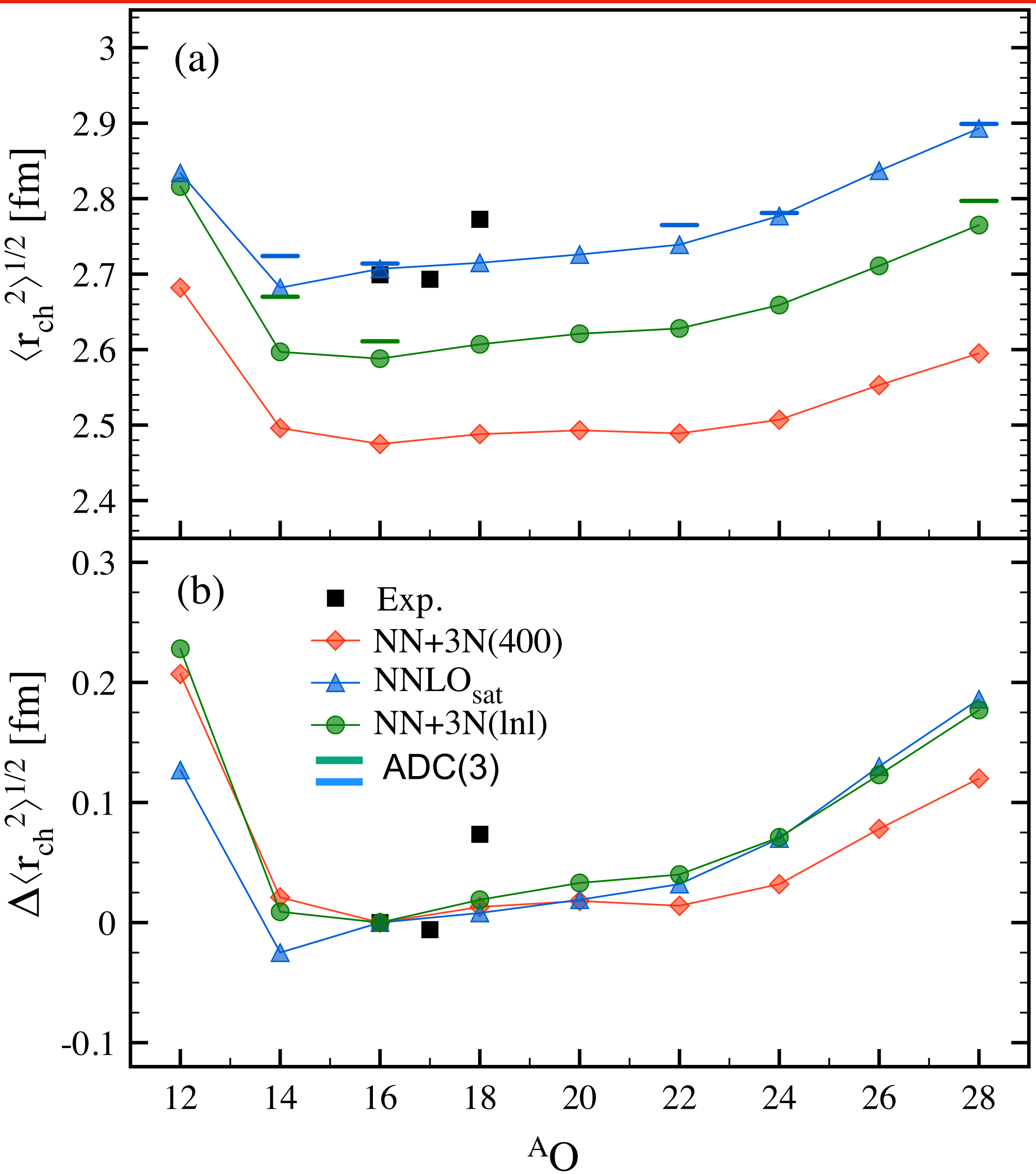

$$\langle r_{\mathrm{ch}}^2\rangle = \langle r_{\mathrm{pt}\text{-}p}^2\rangle + \langle R_p^2\rangle + \frac{N}{Z}\langle R_n^2\rangle + \frac{3\hbar^2}{4m_p^2c^2}$$

$$\langle R_p^2\rangle = 0.8775(51)\ \mathrm{fm}^2$$

$$\langle R_n^2\rangle = -0.1149(27)\ \mathrm{fm}^2$$

- Radii difficult to reproduce for current χEFT Hamiltonians (**NNLO$_{sat}$** fitted to Oxygen)
- **NN+3N(lnl)** improves w.r.t. **NN+3N(400)**
- Relative radii may correct systematic errors (choice of $\hbar\omega$, inconsistent SRG evolution)

Charge radii in Calcium isotopes

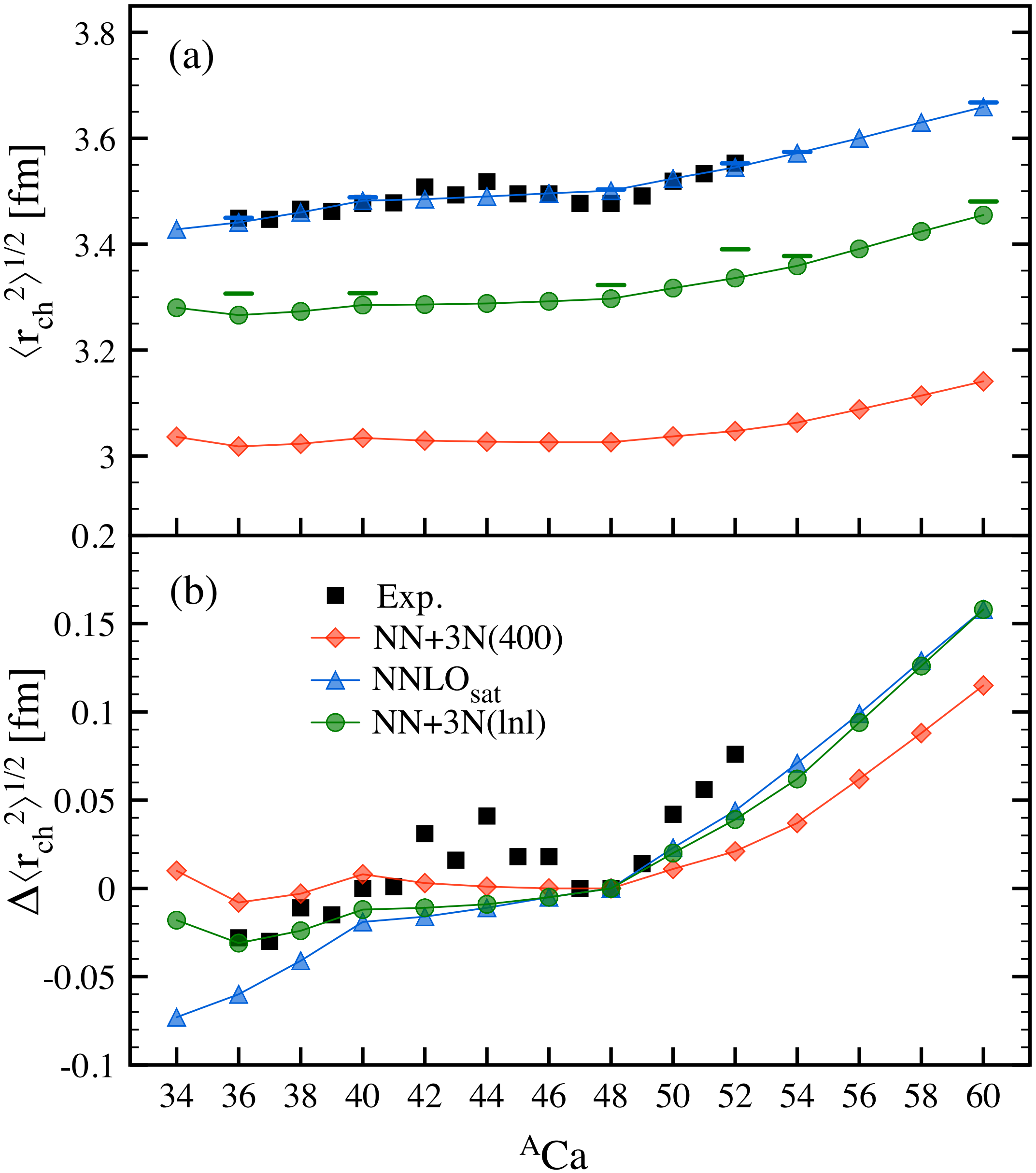

- NN+3N(lnl) improves significantly with respect to NN+3N(400)
- NN+3N(lnl): 5-6% underestimation of experimental values
- Current chiral interaction cannot reproduce radii (unless fitted)

- No account of parabolic trend ^{40}Ca-^{48}Ca (missing high-order *mp-mh* excitations)
- Steep slope leading to ^{52}Ca not reproduced

Charge radii in Nickel isotopes

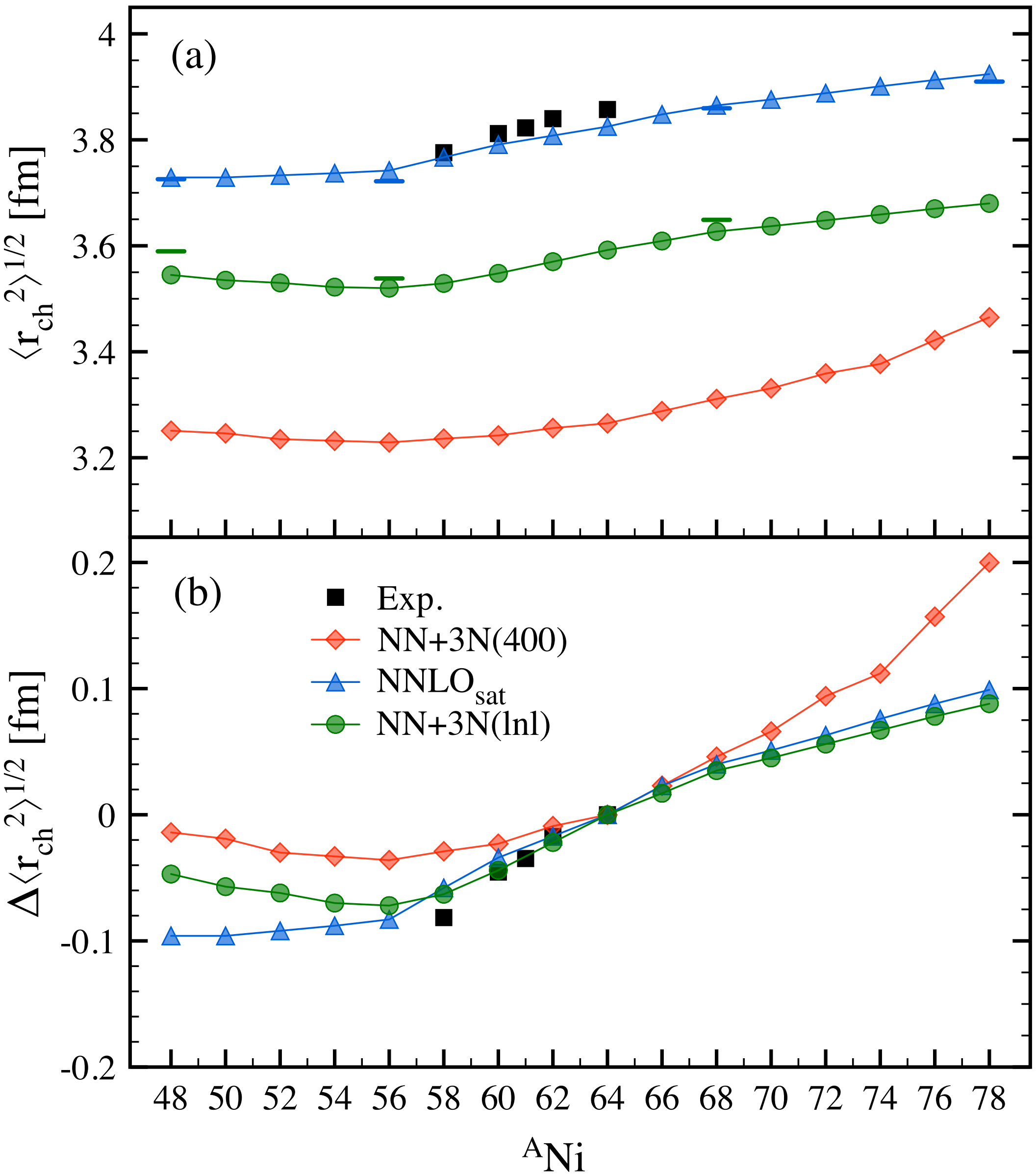

- **NNLO$_{sat}$** maintains good reproduction of charge radii in A~60 region
- Trend of experimental data reproduced
- Predicted kink at ^{56}Ni (signature of shell closure)
- Different trends predicted in the neutron-deficient region

One-neutron addition (^{49}Ca) removal (^{47}Ca) spectra

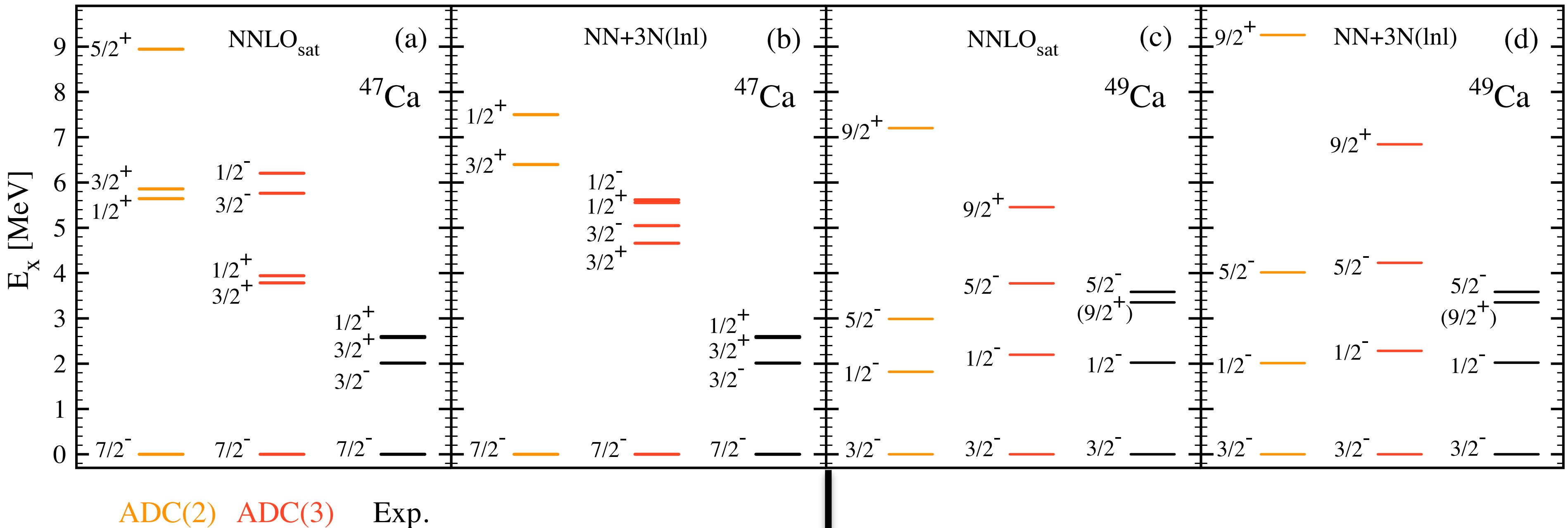

^{47}Ca: $f_{7/2}$ and 1$s_{1/2}$-$d_{3/2}$ levels position

✔ Computed spectra too spread out

- N=20 gap overestimated
- ADC(3) increases levels density

^{49}Ca: *pf*-shell levels position

✔ Agreement with exp. spectra

- N=28 and N=32 gaps under control
- ADC(3) refines splitting

One-nucleon addition (^{55}Ca,^{55}Sc) removal (^{53}Ca,^{53}K) spectra

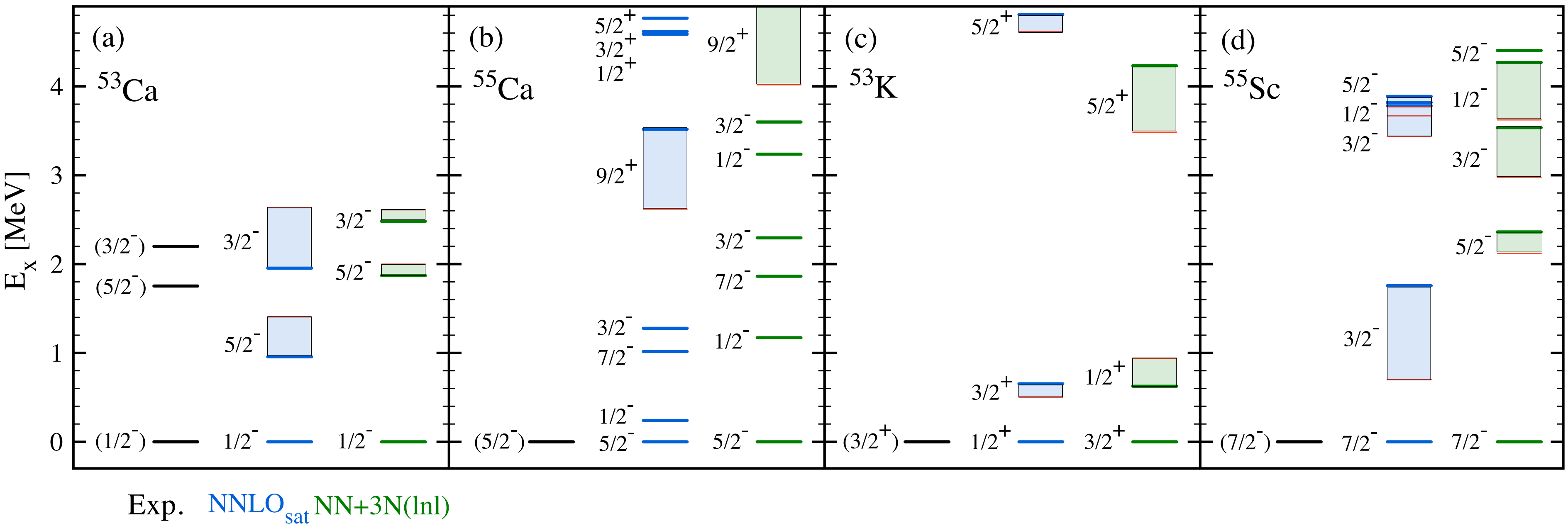

- ADC(3) corrections larger for the harder (no SRG evolution) **NNLO$_{sat}$**

- **NN+3N(lnl)** better than **NNLO$_{sat}$** :
  - ✳ correct splitting in ^{53}Ca
  - ✳ right g.s. spin assignment in ^{53}K

Spectra of K isotopes

Laser spectroscopy of Potassium with COLLAPS @ ISOLDE

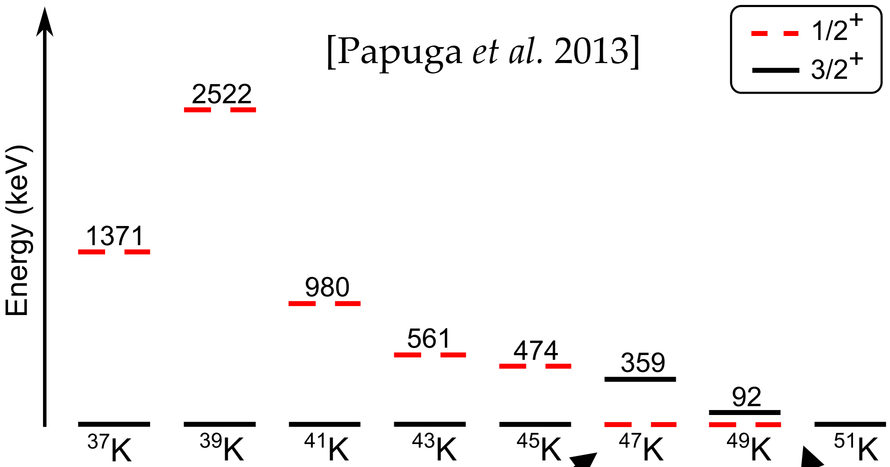

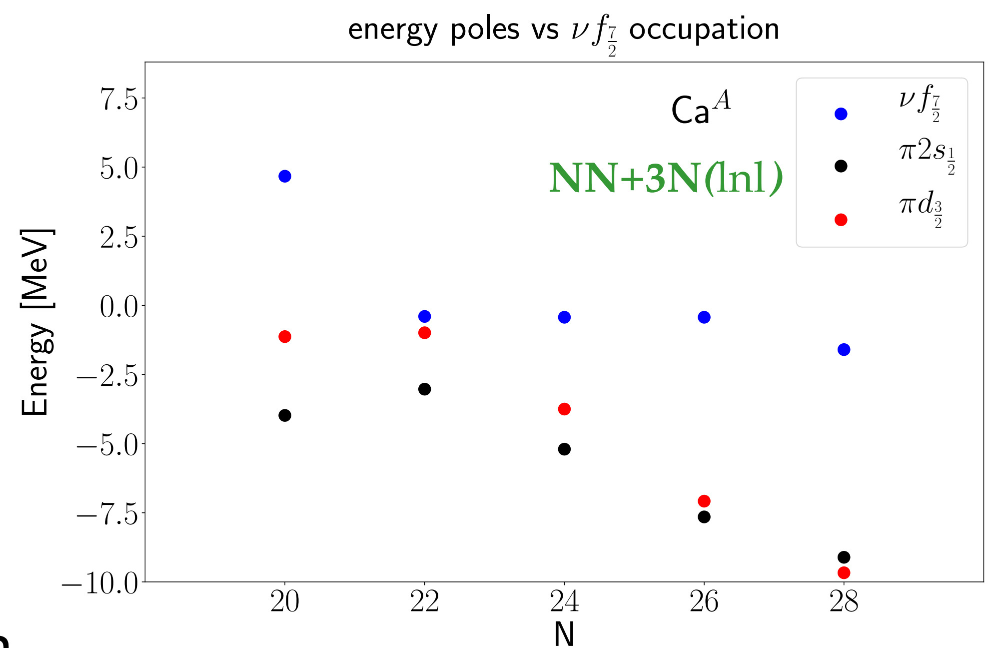

g.s. spin inversion and re-inversion

Tensor force effect
(Otsuka *et al* PRL **95** 232502)

Spectra of K isotopes

Laser spectroscopy of Potassium with COLLAPS @ ISOLDE

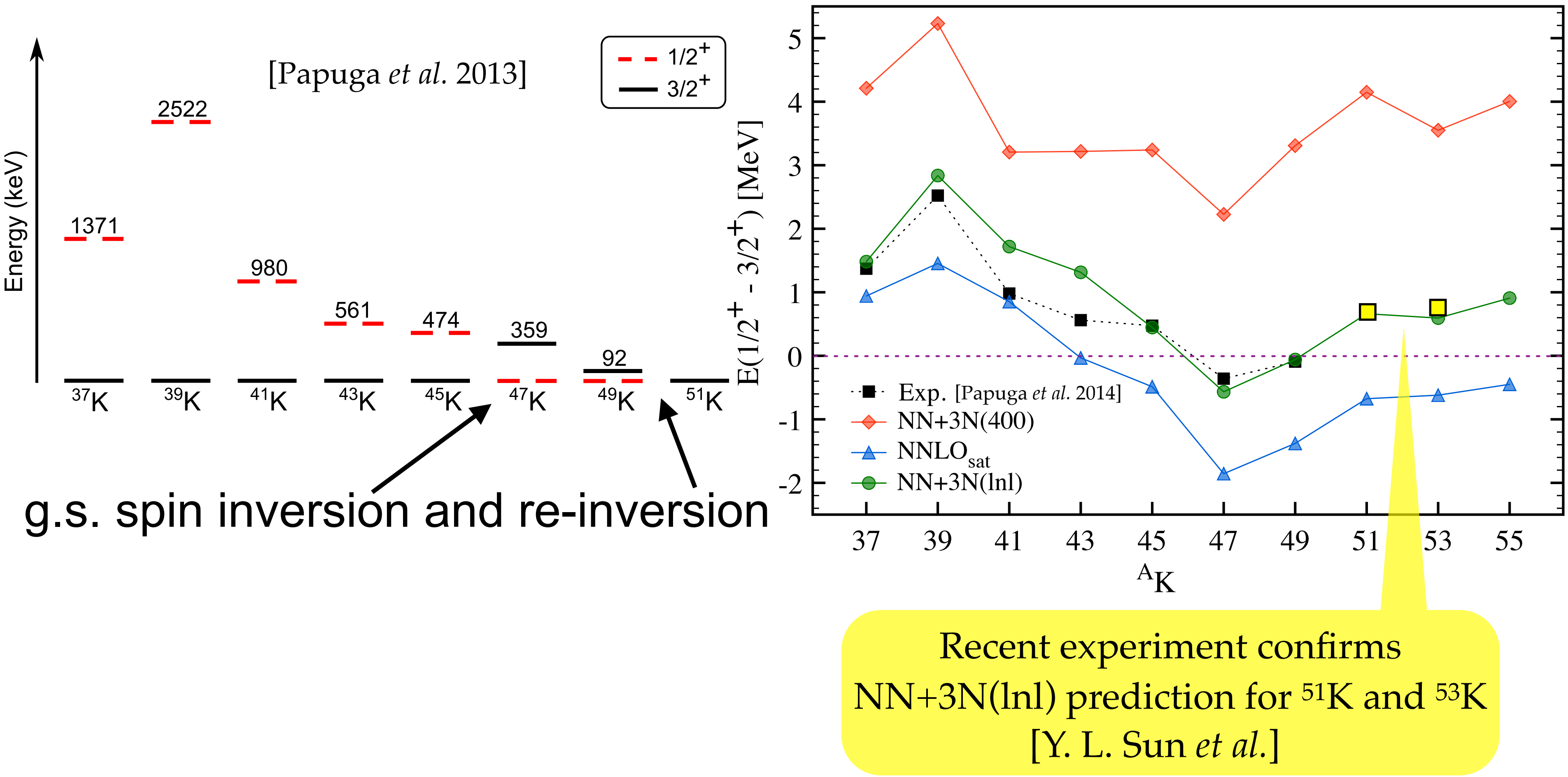

Outline

- Self-consistent Green's function (SCGF) method
  Recent pedagogical review: A. Carbone, C. Barbieri, *Lect. Notes Phys.* 936 (2017)

- Testing χEFT Hamiltonians with SCGF
  V. Somà, P. Navrátil, FR, C. Barbieri, T. Duguet, *arXiv: 1907.09790* (2019)
  - Radii of Oxygen, Calcium and Nickel isotopic chains
  - Spectra of selected Calcium and Potassium isotopes

- Dipole Response Function and Polarisability in medium mass nuclei
  FR, C. Barbieri, *Phys. Rev. C* **99** 054327 (2019)
  - Oxygen isotopes: ^{14}O, ^{16}O, ^{22}O and ^{24}O
  - Calcium isotopes: ^{36}Ca, ^{40}Ca, ^{48}Ca and ^{54}Ca
  - ^{68}Ni

Electromagnetic response in SCGF

OBSERVABLES

$$\sigma_\gamma(E) = 4\pi^2 \alpha E \, R(E)$$ PHOTOABSORPTION CROSS SECTION

$$\alpha_D = 2\alpha \int dE \, \frac{R(E)}{E}$$ ELECTRIC DIPOLE POLARIZABILITY

Response $R(E)$ depends on excited states of the nuclear system, when "probed" with dipole operator $\hat{D}$

$$R(E) = \sum_\nu \left| \boxed{<\psi_\nu^A|\hat{D}|\psi_0^A>} \right|^2 \delta_{E_\nu,E}$$

$$\sum_{ab} <a|\hat{D}|b> <\psi_\nu^A|c_a^\dagger c_b|\psi_0^A>$$

s.p. matrix element of the dipole one-body operator

Nuclear structure component: Transition density matrix

Polarization propagator and Bethe-Salpeter equation

$$\Pi_{\gamma\delta,\alpha\beta}(\omega) = \sum_n \frac{< \Psi_0^A | a_\delta^\dagger a_\gamma | \Psi_n^A > < \Psi_n^A | a_\alpha^\dagger a_\beta | \Psi_0^A >}{\hbar\omega - (E_n^A - E_0^A) + \mathrm{i}\eta}$$

Two-body Propagator

$$\epsilon_n^\pi \equiv E_n^A - E_0^A$$

Energies of the excited states of the A-nucleon system

Equation for the polarization propagator

$$\Pi_{\gamma\delta,\alpha\beta}(\omega) = \Pi^f_{\gamma\delta,\alpha\beta}(\omega) + \Pi^f_{\gamma\delta,\mu\rho}(\omega) K^{(p-h)}_{\mu\sigma,\rho\nu}(\omega) \Pi_{\nu\sigma,\alpha\beta}(\omega)$$

Free polarization Propagator

p-h kernel

Approximated solution of the Bethe-Salpeter equation

$$\Pi_{\gamma\delta,\alpha\beta}(\omega) = \Pi^{f}_{\gamma\delta,\alpha\beta}(\omega) + \Pi^{f}_{\gamma\delta,\mu\rho}(\omega) K^{(p-h)}_{\mu\sigma,\rho\nu}(\omega) \Pi_{\nu\sigma,\alpha\beta}(\omega)$$

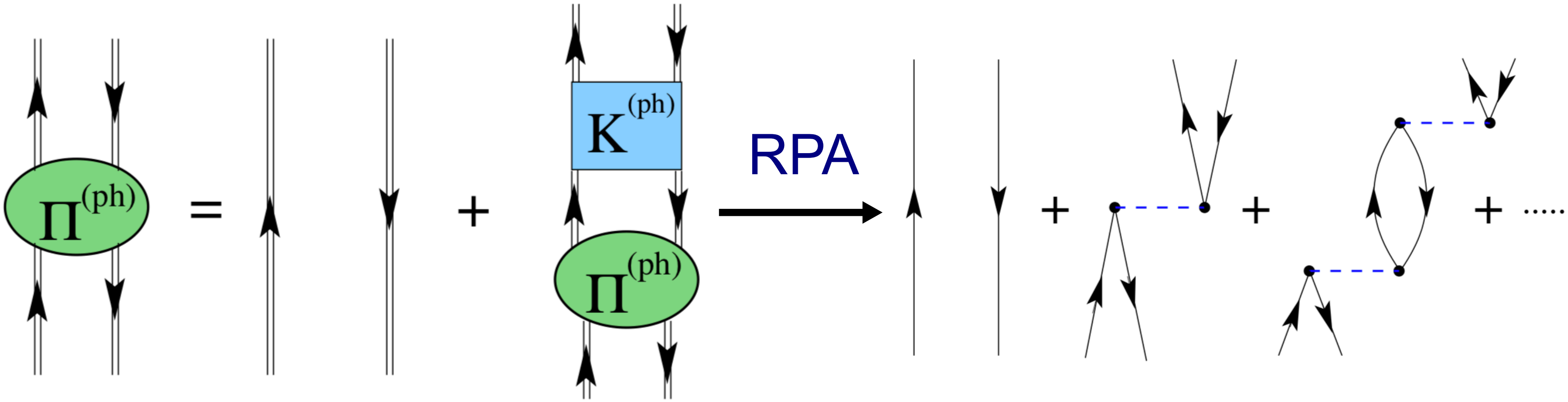

Fig. from PRC 68, 014311 (2003)

Extension of the RPA: 1) Fully-dressed (correlated) single-particle propagator in the RPA diagrams

C. Barbieri, W. Dickhoff PRC 68, 014311 (2003)

2) Reduction of the number of poles of the dressed propagator

C. Barbieri, M. Hjorth-Jensen PRC 79, 064313 (2009)

Features of the calculation

- Dyson (Number conserving) SCGF
- NN and 3N nuclear interaction **NNLO$_{\mathbf{sat}}$**
- Electric dipole operator **E1** $\hat{Q}_{1m}^{T=1} = \frac{N}{N+Z}\sum_{p=1}^{Z} r_p Y_{1m} - \frac{Z}{N+Z}\sum_{n=1}^{N} r_n Y_{1m}$
- Single-particle harmonic oscillator basis (N$_{max}$, $\hbar\omega$)

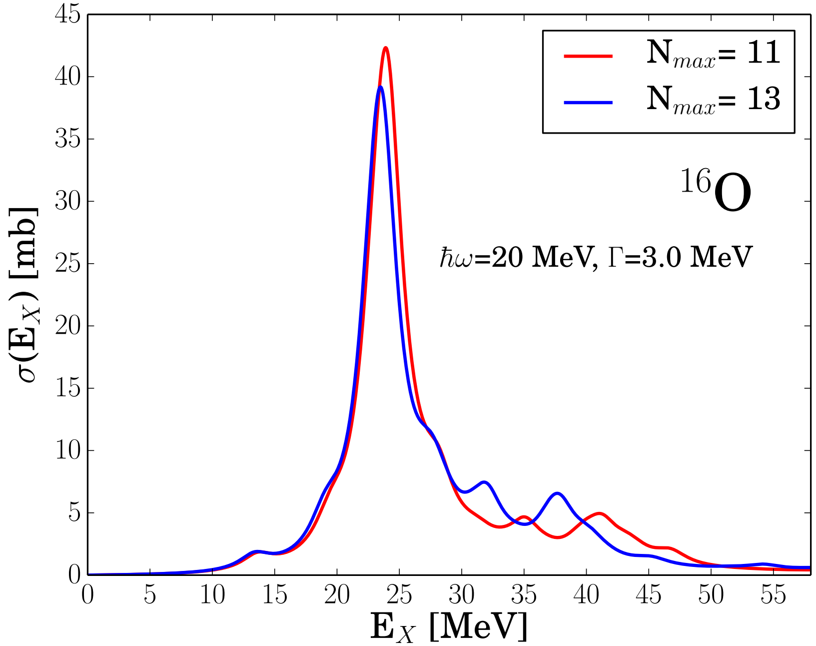

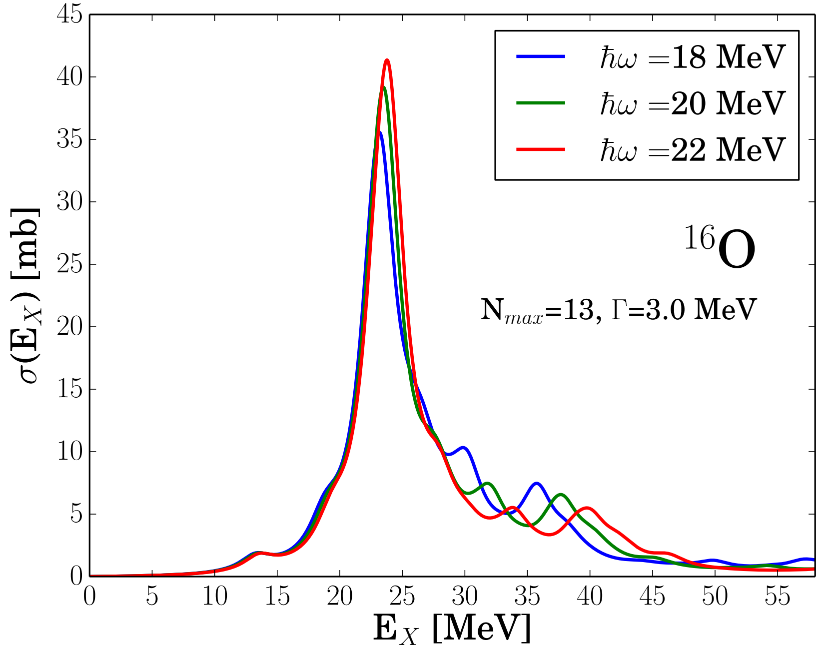

δ(α$_D$, N$_{max}$)=2%

δ(α$_D$, $\hbar\omega$)=1.5%

Discrete spectrum convolution

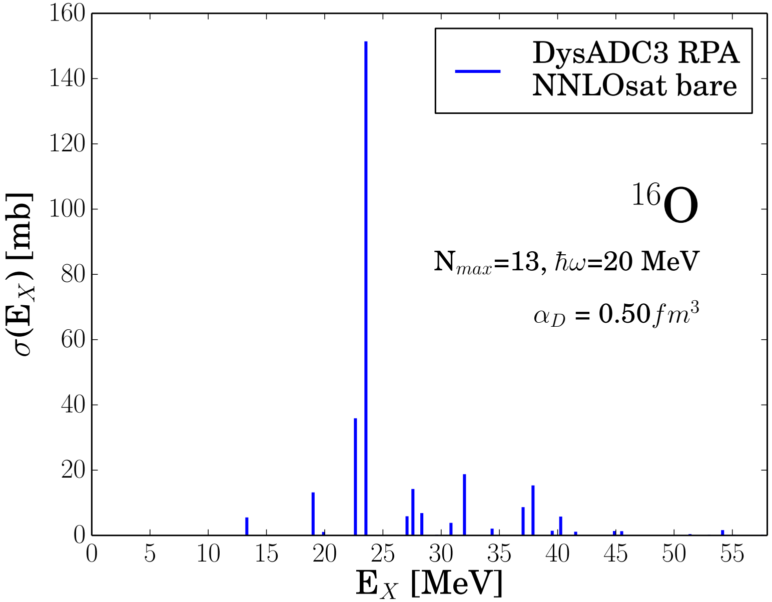

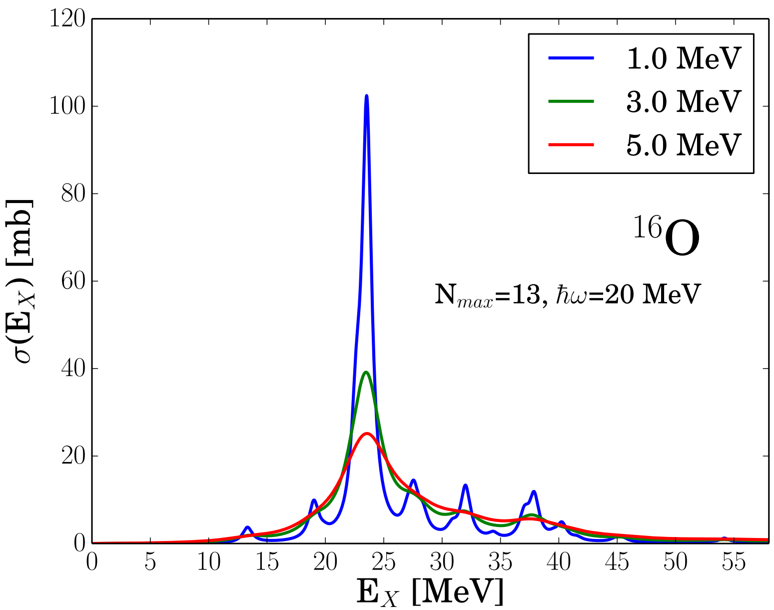

No treatment of the continuum

$$R_\Gamma(E) = \sum_n (\langle \Psi_n^A | \hat{\mathcal{Q}}_{1m}^{T=1} | \Psi_0^A \rangle)^2 \frac{\Gamma/2\pi}{(E_n^A - E)^2 + \Gamma^2/4}$$

Γ width of the Lorentzian

Many-body truncation convergence

Convergence wrt inclusion of correlations in the reference propagator

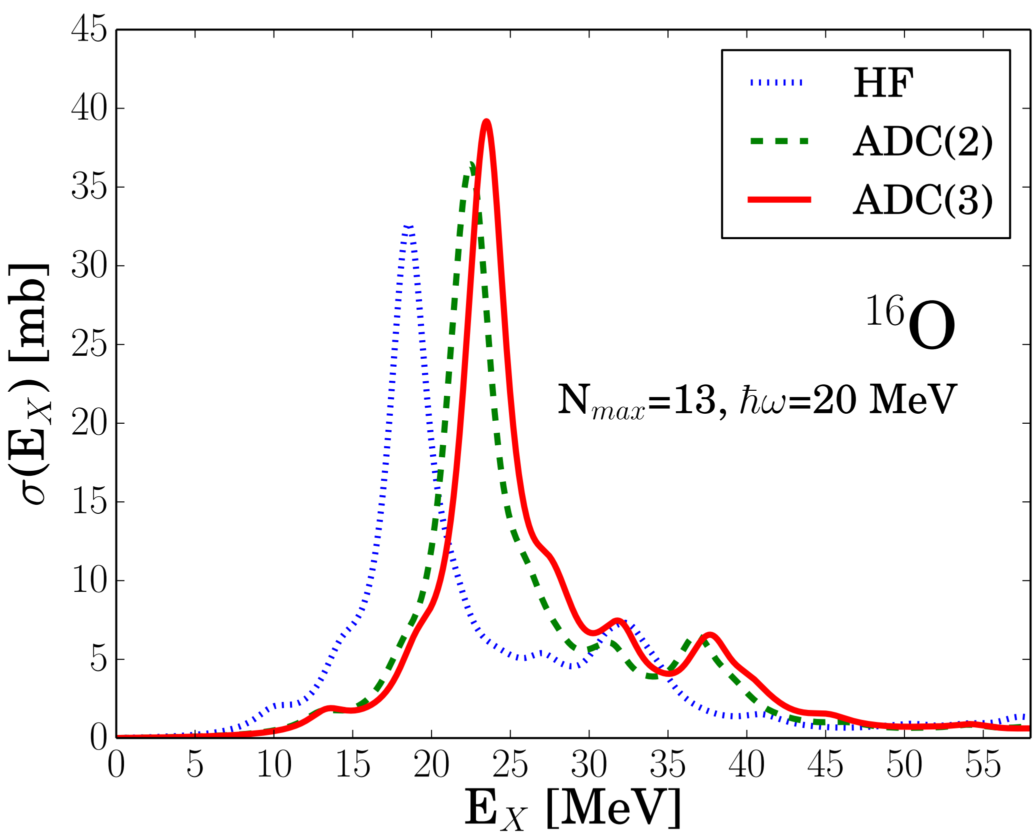

- Impact of correlation beyond mean field
- Towards saturation of correlations from ADC(2) to ADC(3)

Results for Oxygen isotopes

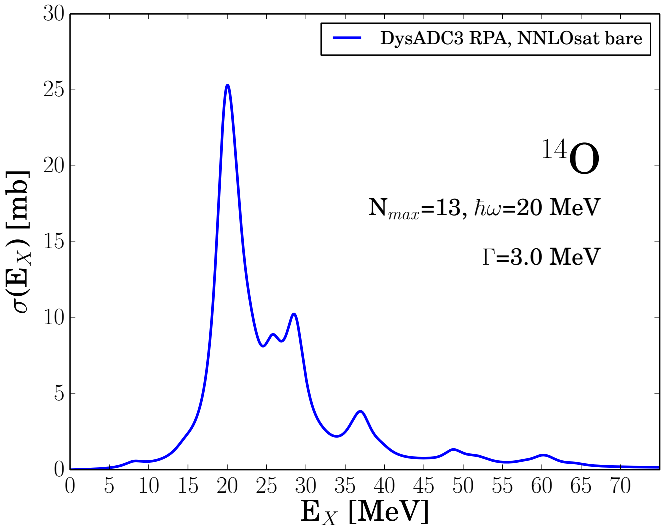

NNLO$_{\text{sat}}$

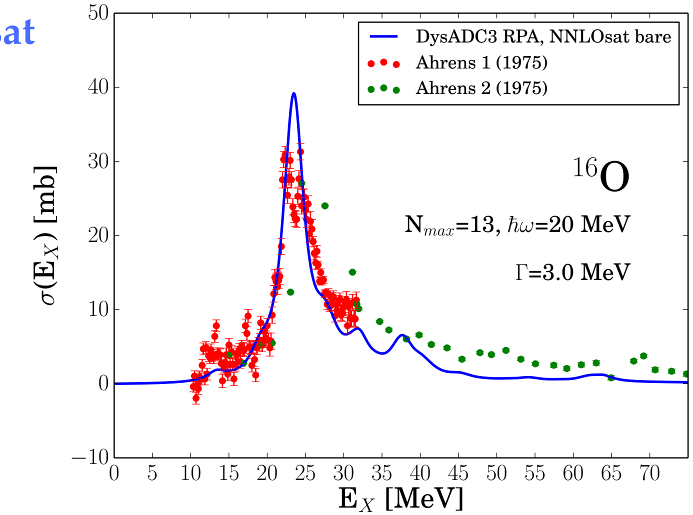

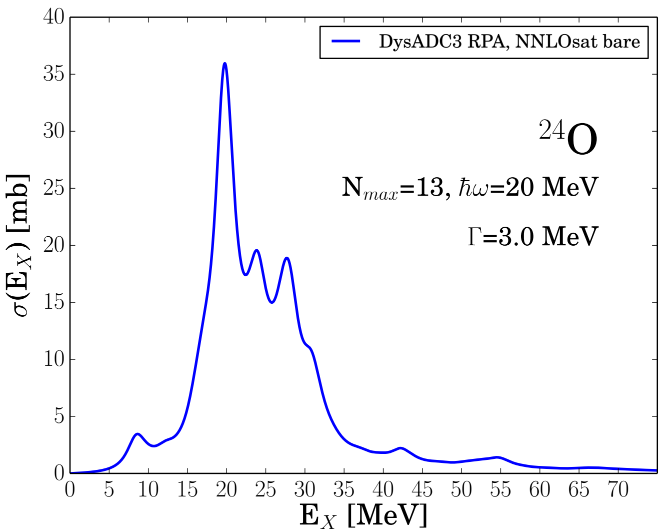

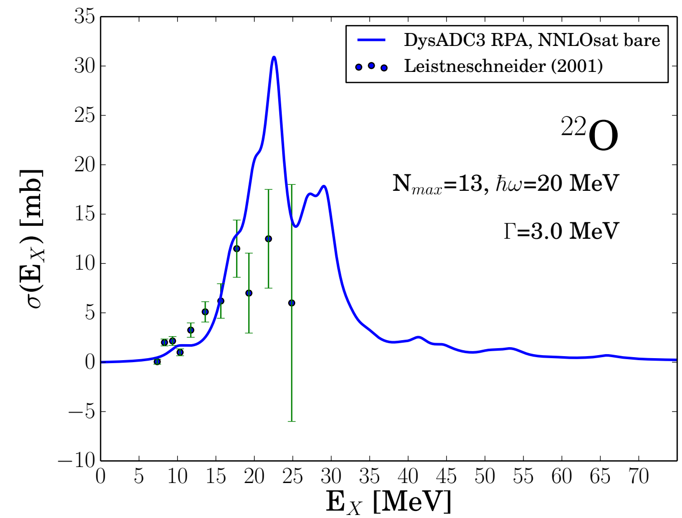

$$\sigma_\gamma(E) = 4\pi^2 \alpha E \, R(E)$$

- GDR position of ^{16}O reproduced
- Hint of a soft dipole mode on the neutron-rich isotope

Polarizability in ^{16}O and ^{22}O

$$\alpha_D = 2\alpha \int dE \, \frac{R(E)}{E}$$

α_D (fm³)	Exp	SCGF	CC-LIT
^{16}O	0.585(9)	0.50	0.57(1) * 0.528 **
^{22}O	0.43(4)	0.72	0.86(4) * na **

$\delta(\alpha_D$, th-exp$) \simeq 15\%$ (^{16}O)

Coupled-Cluster + LIT

M. Miorelli, S. Bacca et al. Phys Rev C 98, 014324 (2018)

* Doubles/Doubles. ** Triples/Triples

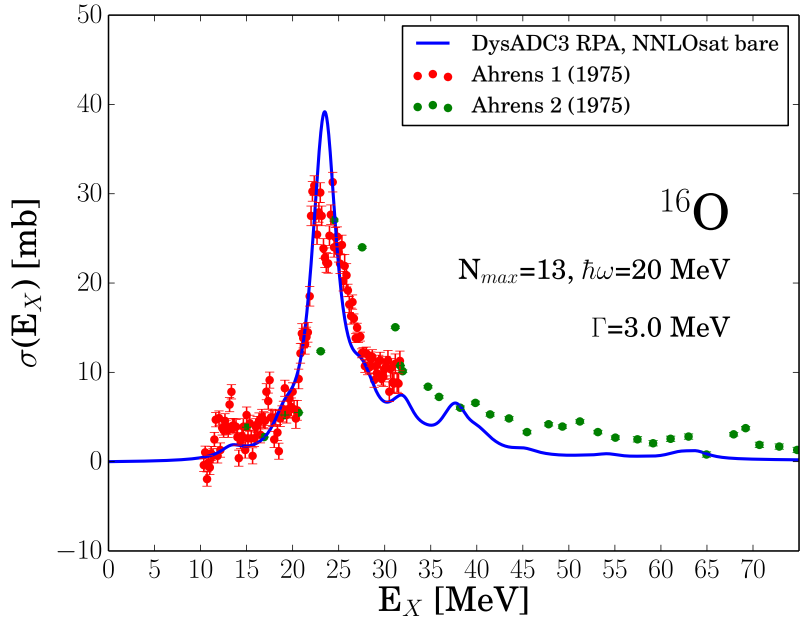

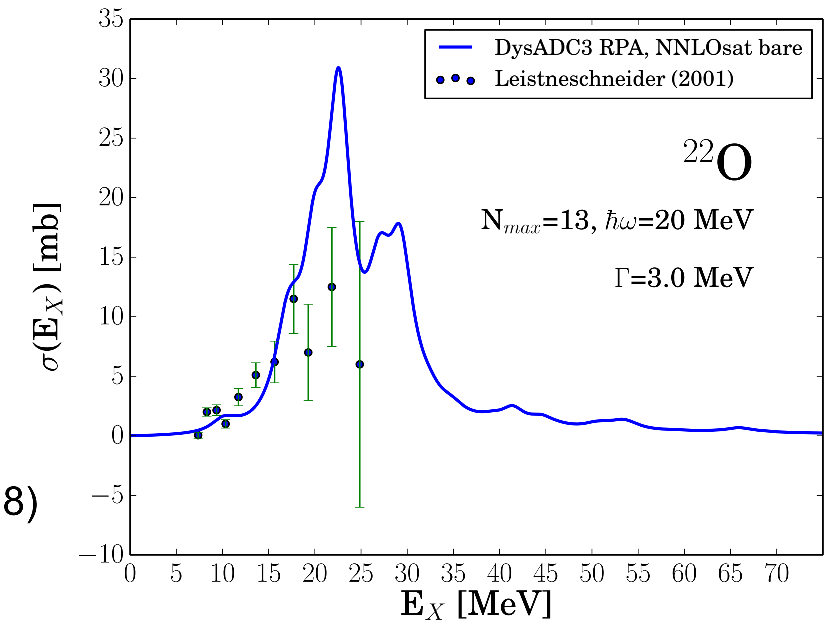

Polarizability in ^{16}O and ^{22}O

$$\alpha_D = 2\alpha \int dE \, \frac{R(E)}{E}$$

α_D (fm^3)	Exp	SCGF	CC-LIT
^{16}O	0.585(9)	0.50	0.57(1) * 0.528 **
^{22}O	0.43(4)	0.72	0.86(4) * na **

$\delta(\alpha_D$, th-exp$) \simeq 15\%$ (^{16}O)

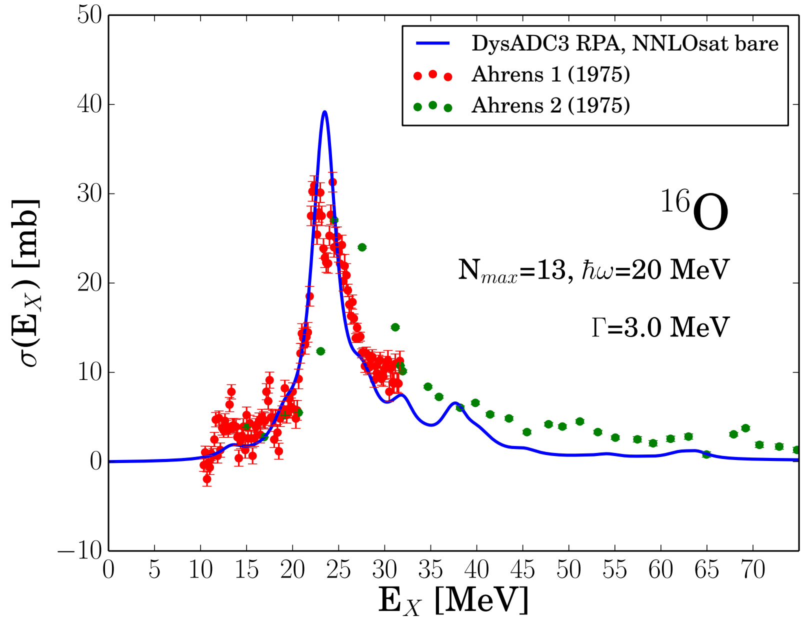

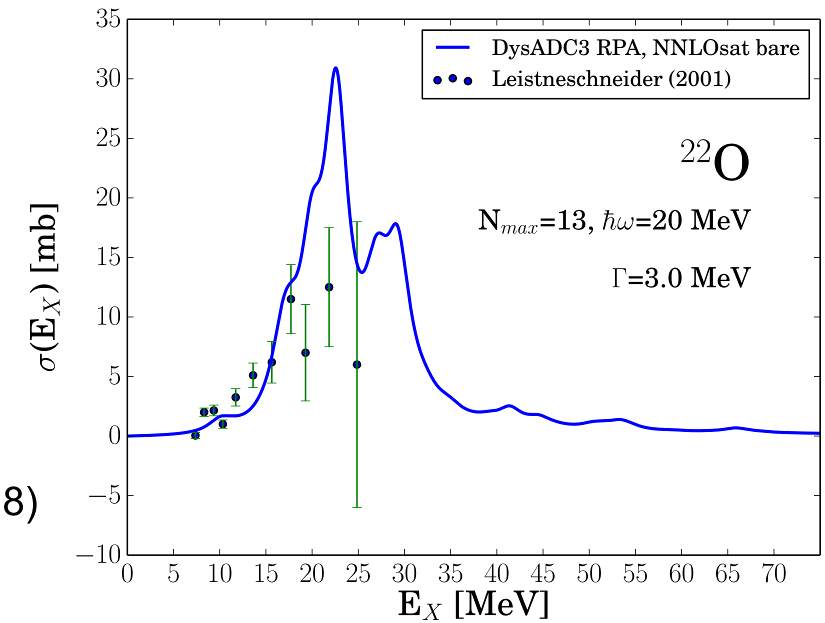

Coupled-Cluster + LIT

M. Miorelli, S. Bacca et al. Phys Rev C 98, 014324 (2018)

* Doubles/Doubles. ** Triples/Triples

Polarizability in ^{16}O and ^{22}O

$$\alpha_D = 2\alpha \int dE \, \frac{R(E)}{E}$$

α_D (fm^3)	Exp	SCGF	CC-LIT
^{16}O	0.585(9)	0.50	0.57(1) * 0.528 **
^{22}O (< 3 MeV)	0.07(2)	0.05	0.05(1) * na **

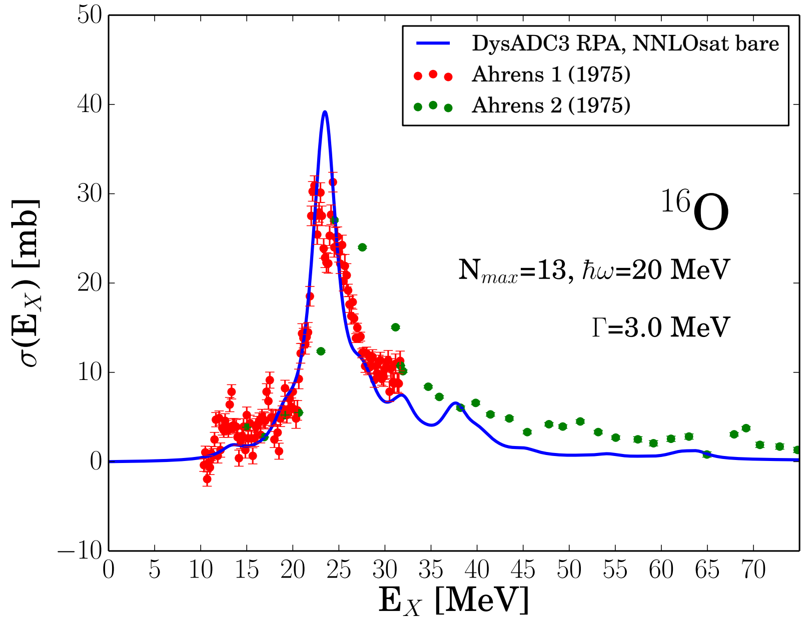

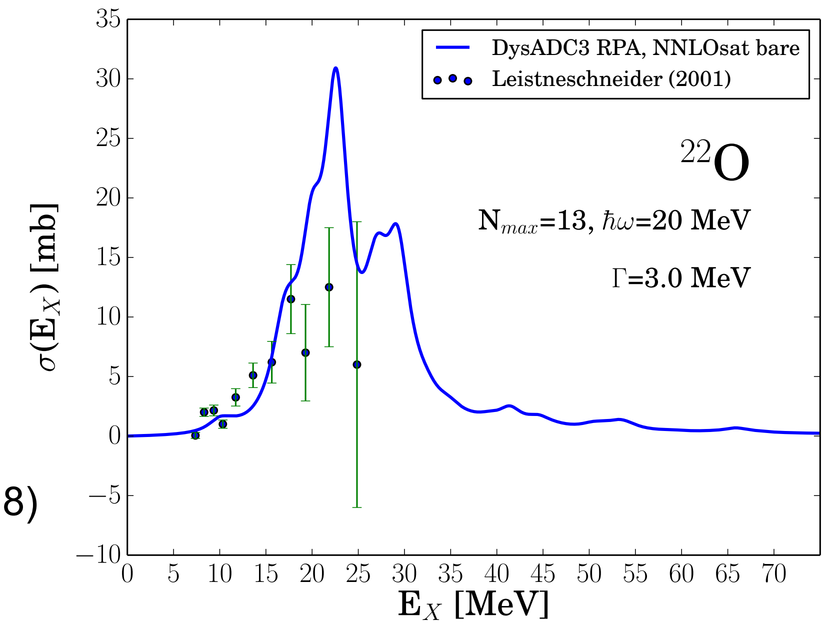

Coupled-Cluster + LIT

M. Miorelli, S. Bacca et al. Phys Rev C 98, 014324 (2018)

* Doubles/Doubles. ** Triples/Triples

Results for Calcium isotopes

$\mathbf{NNLO_{sat}}$

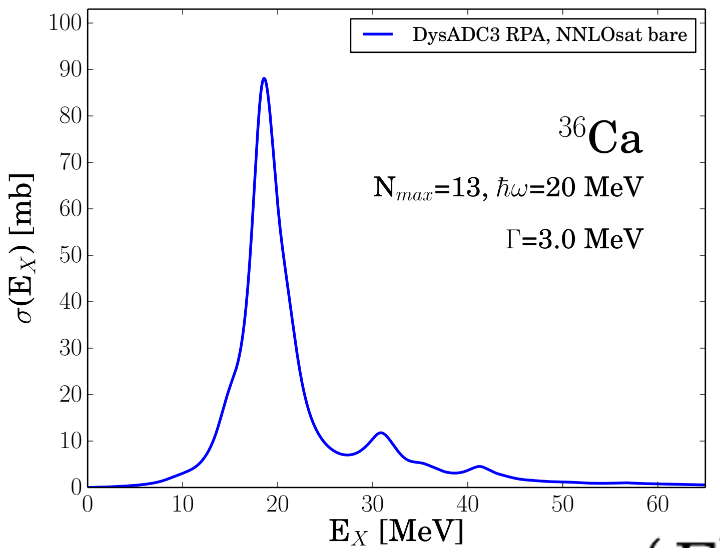

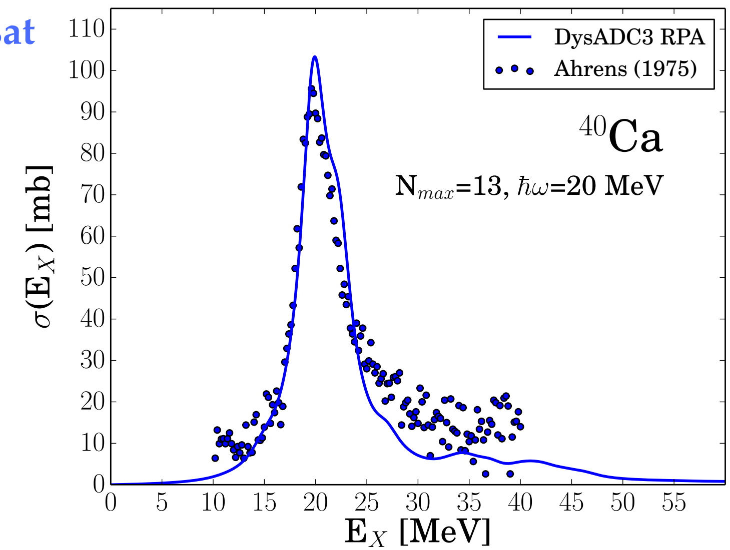

$$\sigma_\gamma(E) = 4\pi^2 \alpha E\, R(E)$$

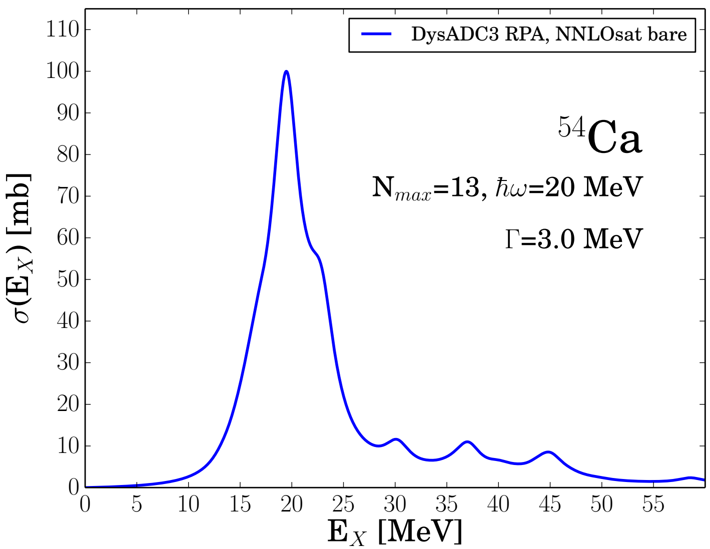

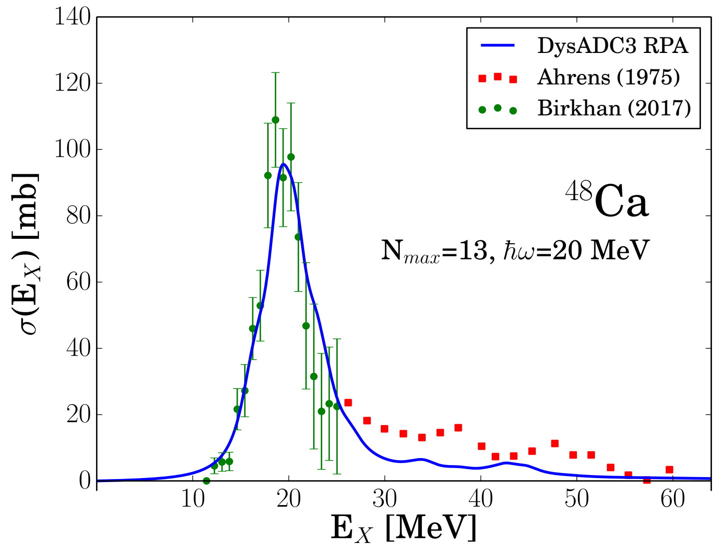

Polarizability in ^{40}Ca and ^{48}Ca

$$\alpha_D = 2\alpha \int dE \, \frac{R(E)}{E}$$

α_D (fm^3)	Exp	SCGF	CC-LIT
^{40}Ca	2.23(3)	1,79	1.87(3) * na **
^{48}Ca	2.07(22) (Birkhan et al)	2.06	2.45 * 2.25(8)**

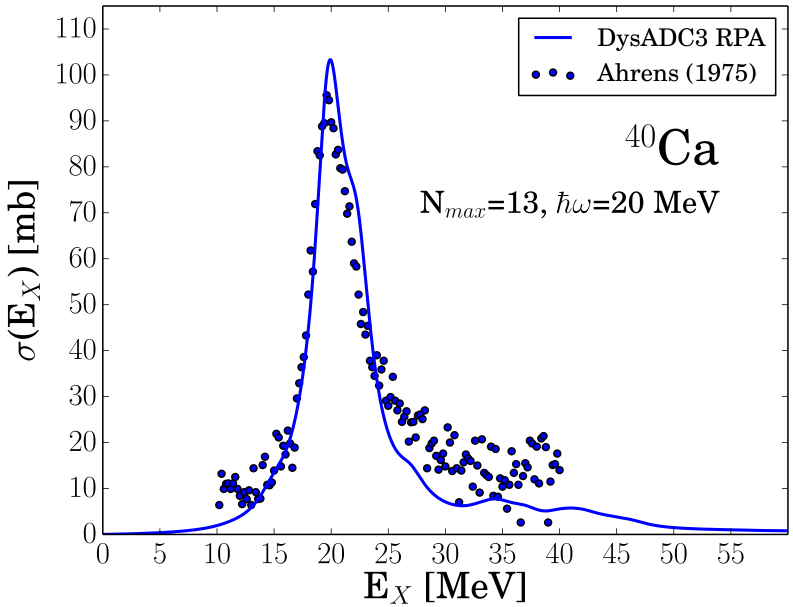

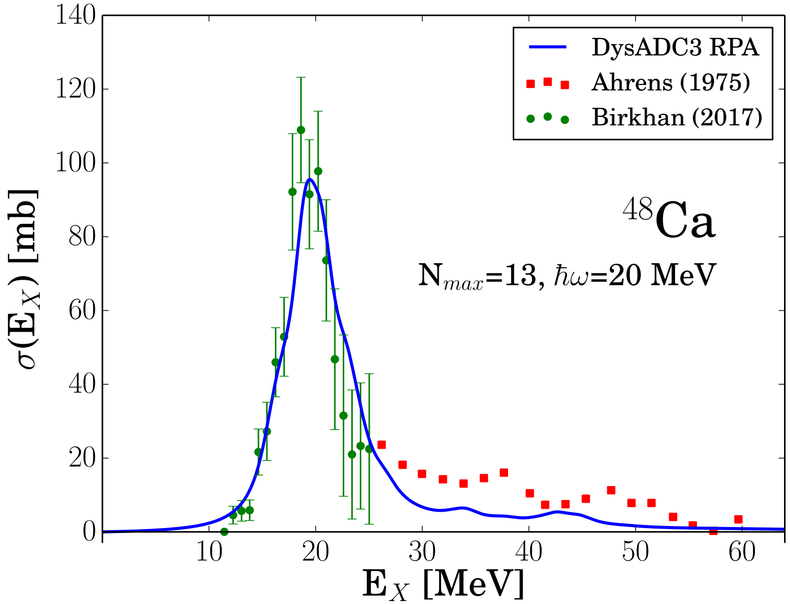

Coupled-Cluster + LIT

M. Miorelli et al. Phys Rev C 98, 014324 (2018)

* Doubles/Doubles. ** Triples/Triples

Results for ^{68}Ni

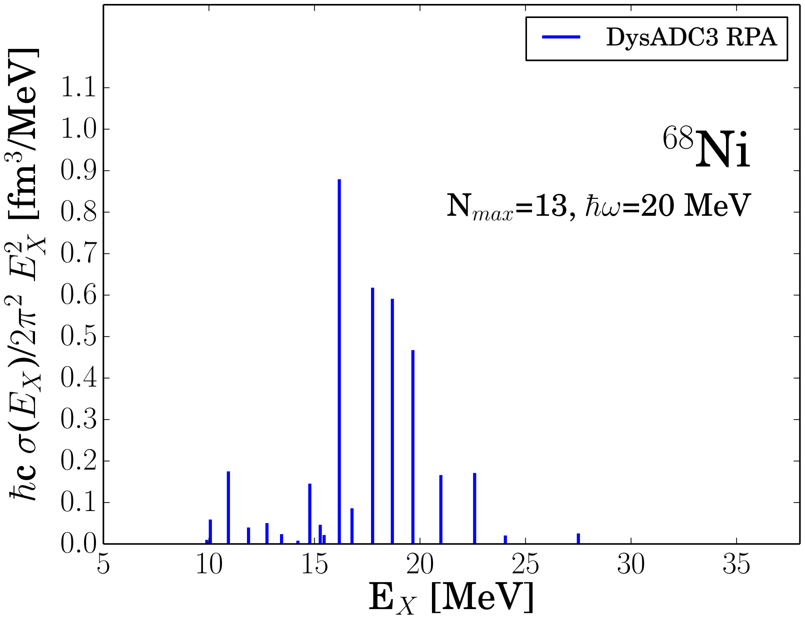

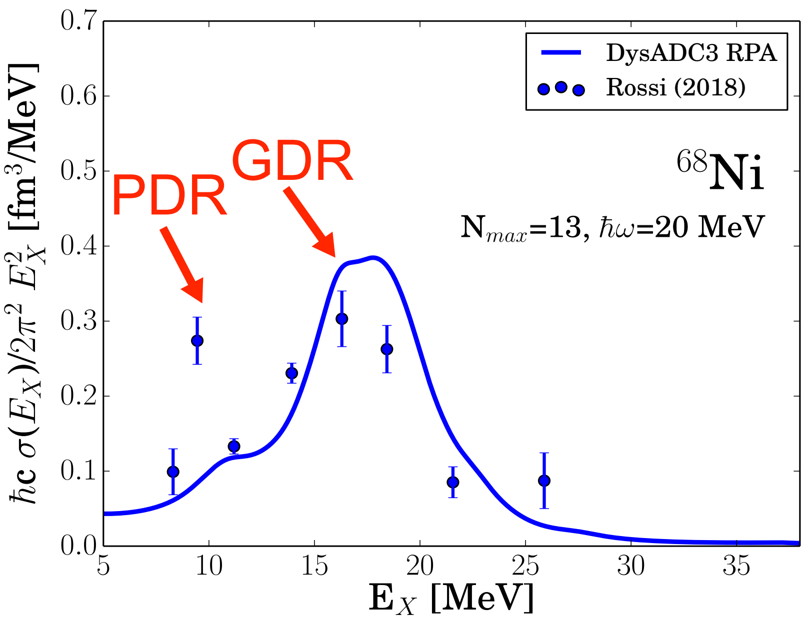

Comparison with experimental Coulomb excitation

(Rossi *et al* PRL, 111, 242503 (2013))

	Exp	SCGF
Pigmy (MeV)	9.55(17)	10.68 10.92
Giant (MeV)	17.1(2)	18.10
α_D (fm³)	3.88(31)	3.60 NNLO$_{sat}$ 2.72 *NN*+3*N*(lnl)

$\delta(\alpha_D$, th-exp$) \simeq 7\%$

Conclusions/Perspectives

Interaction bigger source of theoretical error
(especially for radii and excitation spectra):

- “Universal” Hamiltonian for medium-mass calculations not available yet
- Pragmatical approach

Many-body formalism developments:

- Overcome the many-body combinatorics: Code optimisation, Importance truncation, Tensor factorisation
  - ➡ improve convergence and scope of the method (towards heavy nuclei)
- Extend the many-body expansion:
  - Horizontal expansion: restore U(1) ➡ static correlations
    break SU(2) ➡ deformed nuclei (odd-odd)
  - Vertical expansion: ADC(3)
    Autom. diagr. generation ➡ dynamical correlations

Collaborators

SCGF project:

Carlo Barbieri (University of Surrey)
Thomas Duguet (CEA Saclay)
Petr Navrátil (TRIUMF)
Vittorio Somà (CEA Saclay)

CEA Saclay group:

Pierre Arthuis (University of Surrey)
Mikael Frosini
Raphaël Lasseri
Andrea Porro (Università di Milano)
Julien Ripoche
Alexander Tichai